COMPLEX GEOMETRICAL OPTICS SOLUTIONS AND RECONSTRUCTION OF DISCONTINUITIES

GUNTHER UHLMANN AND JENN-NAN WANG

Abstract. In this paper we provide a framework for constructing general complex geometrical optics solutions for several systems of two variables that can be reduced to a system with the Laplacian as the leading order term. We apply these special solutions to the problem of reconstructing inclusions inside of a domain filled with known conductivity from local boundary measurements. Computational results demonstrate the versatility of these solutions to determine electrical inclusions.

1. Introduction

Inverse boundary value problems are a class of inverse problems where one attempts to determine the internal parameters of body by making measurements only at the surface of the body. A prototypical example that has received a lot of attention is Electrical Impedance Tomography (EIT). In this inverse method one would like to determine the conductivity distribution inside a body by making voltage and current measurements at the boundary. This is also called Calderón problem [2]. The boundary information is encoded in the Dirichlet to Neumann map associated to the conductivity equation. Sylvester and Uhlmann [23] constructed complex geometrical optics (CGO) solutions for the conductivity equation. The phase functions of these solutions are linear. CGO optics have been used in EIT and have been instrumental in solving several inverse problems. We will not review these developments in detail here; see [25] and [24] for references; other reviews in EIT are [1] and [3]. There are many applications of EIT ranging from early breast cancer detection [27] to geophysical sensing for underground objects, see [14, 19, 20, 22]. The article [23] and the ones reviewed in [24] assumes that the measurements are made on the whole boundary. However, it is often possible to make the measurements only

The first author was partially supported by NSF and a Walker Family Endowed Professorship.

The second author was supported in part by the National Science Council of Taiwan (NSC 95-2115-M-002-003).

on part of the boundary; this is the partial data problem. This is the case for the applications in breast cancer detection and geophysical sensing mentioned above. Recently, new CGO solutions that are useful for the partial data problem were constructed in [16] for the conductivity equation and zeroth order perturbations of the Laplacian. The real part of the phase of these solutions are limiting Carleman weights. They have been generalized to first order perturbation of the Laplacian for scalar equations or systems in [4], [6], [21], and [26]. Constructions of CGO solutions for the conductivity equation and zeroth order perturbations of the Laplacian using hyperbolic geometry can be found in [13]; these have been applied to determine electrical inclusions in [7].

In two dimensions, when the underlying equation has the Laplacian as the leading part, due to the rich conformal structure, we have more freedom of choosing the complex phases for the CGO solutions. In particular any harmonic function is a limiting Carleman weight and can be the real part of a CGO solution. The aim of the paper is to provide a framework for constructing these solutions for several systems of two variables that can be reduced to a system with the Laplacian as the leading term. We apply these special solutions to the problem of reconstructing inclusions inside of a domain filled with known conductivity from local boundary measurements. We also provide numerical results to demonstrate the applicability and flexibility of these special solutions.

Assume that Ω is an open bounded domain in $\mathbb{R}^2$ with smooth boundary. Let $n \in \mathbb{N}$ and denote $U(x) = (u_1(x_1, x_2), \cdots, u_n(x_1, x_2))^\top$. We consider the following system of equations:

$$PU := \Delta_x U + A_1(x)\partial_{x_1} U + A_2(x)\partial_{x_2} U + Q(x)U = 0 \quad \text{in} \quad \Omega, \quad (1.1)$$

where $\Delta_x = \partial_{x_1}^2 + \partial_{x_2}^2$ and A_1, A_2, Q are $n \times n$ matrices whose regularities will be specified later. The system (1.1) contains all scalar or two-dimensional physical systems that can be reduced to a system with the Laplacian as the leading part. Those systems include the conductivity equation, the magnetic Schrödinger equation, the two-dimensional isotropic elasticity system, and the two-dimensional Stokes system, etc. In this paper we first study CGO solutions with special phase functions for (1.1).

In the papers [16] [4], [6], [7], [13], [21], and [26], the real part of the phase functions are radial functions. These can be used to probe the region with spherical fronts, the so-called complex spherical waves. Even though these solutions are better suited for the local data problem than the usual CGO solutions with linear phase functions, they are still quite restrictive. Fortunately, in the two dimensional case, we

have many more choices of phase functions. For example, let $\varphi(x)$ be a harmonic function with nonvanishing gradient in Ω, then $\varphi+i\psi$ can the phase function of the CGO solutions when ψ is a harmonic conjugate of φ. In other words, $\rho(x) := \varphi(x) + i\psi(x)$ is holomorphic in Ω. Our method in this paper is developed based on this idea.

Using the CGO solutions, we can consider the problem of finding embedded inclusions in a known medium. This is object identification problem. The method developed here shares the same spirit as Ikehata's *enclosure method* [8]. For the two-dimensional problem, we would like to mention a very interesting result by Ikehata in [10] where he introduced the Mittag-Leffler function in the object identification problem. This has the property that its modulus grows exponentially in some cone and decays to zero algebraically outside the same cone. Using the Mittag-Leffler function and shrinking the opening angle of the cone, one can reconstruct precisely the shapes of some embedded objects such as star-shaped objects. The numerical implementation of the Mittag-Leffler functions was carried out by Ikehata and Siltanen in [11]. The main restriction of the method using the Mittag-Leffler function is that it can be only applied to scalar equations with homogeneous background. That is, they probe the region with harmonic functions.

The novelty of our method is its flexibility in treating scalar equations, or even two-dimensional systems, with inhomogeneous background. Furthermore, for the object identification problem in such general systems, we are able to achieve for these general systems the analogous results as those in [10] and [11] for the conductivity equation with homogeneous background. We would also like to point out that the Mittag-Leffler function is in the form of infinite series. Therefore, to implement the Mittag-Leffler function numerically, one needs first to do a suitable truncation. This clearly introduces *a priori* errors in the input (Dirichlet) data. On the other hand, our special CGO solutions are in closed form. So we can prescribe the exact Dirichlet data in the inverse problem using our method.

Before going further, we also would like to compare our method and that in [7]. As we have pointed out above, the real parts of the phase functions of CGO solutions in [7] are radially symmetric. So their probing fronts are circles or spheres. Moreover, the construction of CGO solutions in [7] is based on the hyperbolic geometry. It has not been developed to studying more general equations or systems. The advantage of our method lies in the freedom of choosing the phase functions of CGO solutions. One useful example is to take $\rho(x)$ as a polynomial. By increasing the degree of the polynomial, we can narrow our probing

fronts. Consequently, we are able to determine more information in the object identification problem in the two dimensional case than [7] does. On the other hand, since the real parts of the phase functions in our CGO solutions are not necessarily radially symmetric, we can create different probing fronts by simply rotating the phase functions.

Like [7], we can also localize the measurements in an arbitrarily small region on the boundary. Our construction of CGO solutions with more general phases is rather elementary. The main idea is to transform CGO solutions with linear phases by suitable conformal mappings. The construction of CGO solutions with linear phases for (1.1) was first given by Nakamura and Uhlmann in [17], [18] where they introduced the intertwining technique in handling the first order terms (also see [5] for similar results). Here we shall use Carleman's technique to construct CGO solutions with linear phases for (1.1).

This paper is organized a follows. In Section 2, we give concrete examples of (1.1). In Section 3, we review of the construction of CGO solutions with linear phases for (1.1). CGO solutions with more general phases will be discussed in Section 4. For an application of CGO solutions with general phases, we consider the problem of reconstructing inclusions embedded in a domain with known conductivity by boundary measurements. Numerical experiments of our method are presented in Section 6.

2. Physical examples of (1.1)

2.1. **Conductivity equation.** Our first example is the well-known conductivity equation. Let $\gamma(x) \in C^2(\bar{\Omega})$ and $\gamma(x) > 0$ for all $x \in \bar{\Omega}$. We consider the equation:

$$\nabla \cdot (\gamma \nabla u) = 0 \quad \text{in} \quad \Omega. \tag{2.1}$$

Introducing the new variable $v = \gamma^{1/2} u$, (2.1) is equivalent to

$$(\Delta + q)v = 0 \quad \text{in} \quad \Omega \tag{2.2}$$

with $q = -\Delta\gamma^{1/2}/\gamma^{1/2} \in L^\infty(\Omega)$. (2.2) is a Schrödinger-type equation. We can also consider a more general Schrödinger-type equation with convection term:

$$(\Delta + a(x) \cdot \nabla + q)v = 0 \quad \text{in} \quad \Omega, \tag{2.3}$$

where $a = (a_1, a_2)$.

2.2. **Isotropic elasticity.** The domain Ω is now modeled as an inhomogeneous, isotropic, elastic medium characterized by the Lamé parameters $\lambda(x)$ and $\mu(x)$. Assume that $\lambda(x) \in C^2(\overline{\Omega})$, $\mu(x) \in C^4(\overline{\Omega})$ and the following inequalities hold

$$\mu(x) > 0 \quad \text{and} \quad \lambda(x) + 2\mu(x) > 0 \quad \forall\, x \in \overline{\Omega} \quad \text{(strong ellipticity)}. \tag{2.4}$$

We consider the static isotropic elasticity system without sources

$$\nabla \cdot (\lambda(\nabla \cdot u)I + 2\mu S(\nabla u)) = 0 \quad \text{in} \quad \Omega. \tag{2.5}$$

Here and below, $S(A) = (A + A^T)/2$ denotes the symmetric part of the matrix $A \in \mathbb{C}^{2\times 2}$. Equivalently, if we denote $\sigma(u) = \lambda(\nabla \cdot u)I + 2\mu S(\nabla u)$ the stress tensor, then (2.5) becomes

$$\nabla \cdot \sigma = 0 \quad \text{in} \quad \Omega.$$

On the other hand, since the Lamé parameters are differentiable, we can also write (2.5) in the non-divergence form

$$\mu \Delta u + (\lambda + \mu)\nabla(\nabla \cdot u) + \nabla\lambda \nabla \cdot u + 2S(\nabla u)\nabla\mu = 0 \quad \text{in} \quad \Omega. \tag{2.6}$$

We will use the reduced system derived by Ikehata [9]. This reduction was also mentioned in [24]. Let $\begin{pmatrix} w \\ g \end{pmatrix}$ satisfy

$$\Delta \begin{pmatrix} w \\ g \end{pmatrix} + A(x) \begin{pmatrix} \nabla g \\ \nabla \cdot w \end{pmatrix} + Q(x) \begin{pmatrix} w \\ g \end{pmatrix} = 0, \tag{2.7}$$

where

$$A(x) = \begin{pmatrix} 2\mu^{-1/2}(-\nabla^2 + \Delta)\mu^{-1} & -\nabla \log \mu \\ 0 & \frac{\lambda+\mu}{\lambda+2\mu}\mu^{1/2} \end{pmatrix}$$

and

$$Q(x) = \begin{pmatrix} -\mu^{-1/2}(2\nabla^2 + \Delta)\mu^{1/2} & 2\mu^{-5/2}(\nabla^2 - \Delta)\mu\ \nabla\mu \\ -\frac{\lambda-\mu}{\lambda+2\mu}(\nabla\mu^{1/2})^T & -\mu\Delta\mu^{-1} \end{pmatrix}.$$

Here $\nabla^2 f$ is the Hessian of the scalar function f. Then

$$u := \mu^{-1/2}w + \mu^{-1}\nabla g - g\nabla\mu^{-1}$$

satisfies (2.6). A similar form was also used in [5] for studying the inverse boundary value problem for the isotropic elasticity system.

2.3. **Stokes system.** Let $\mu(x) \in C^4(\bar{\Omega})$ and $\mu(x) > 0$ for all $x \in \bar{\Omega}$. Here μ is called the viscosity function. Suppose that $u = (u_1, u_2)$ and p satisfy the Stokes system:

$$\begin{cases} \nabla \cdot (\mu S(\nabla u)) - \nabla p = 0 \quad \text{in} \quad \Omega, \\ \nabla \cdot u = 0 \quad \text{in} \quad \Omega. \end{cases} \tag{2.8}$$

Here u and p represent the velocity field and the pressure, respectively. Motivated by the isotropic elasticity, we set $u = \mu^{-1/2} w + \mu^{-1} \nabla g - (\nabla \mu^{-1}) g$ and

$$p = \nabla \mu^{1/2} \cdot w + \mu^{1/2} \nabla \cdot w + 2\Delta g = \nabla \cdot (\mu^{1/2} w) + 2\Delta g, \tag{2.9}$$

then (u, p) is a solution of (2.8) provided $\begin{pmatrix} w \\ g \end{pmatrix}$ satisfies

$$\Delta \begin{pmatrix} w \\ g \end{pmatrix} + A(x) \begin{pmatrix} \nabla g \\ \nabla \cdot w \end{pmatrix} + Q(x) \begin{pmatrix} w \\ g \end{pmatrix} = 0 \tag{2.10}$$

with

$$A(x) = \begin{pmatrix} -2\mu^{1/2} \nabla^2 \mu^{-1} & -\mu^{-1} \nabla \mu \\ 0 & \mu^{1/2} \end{pmatrix}$$

and

$$Q = \begin{pmatrix} -2\mu^{-1/2} \nabla^2 \mu^{1/2} - \mu^{-1/2} \Delta \mu^{1/2} & -4\nabla^2 \mu^{-1} \nabla \mu^{1/2} - 2\mu^{1/2} \nabla \cdot (\nabla \mu^{-1}) \\ \mu (\nabla \mu^{-1/2})^T & -\mu \Delta \mu^{-1} \end{pmatrix}.$$

3. CGO solutions with linear phases

In this section we review the method of constructing CGO solutions with linear phases using Carleman estimates. We consider a slightly different system here. Let $\tilde{\Omega}$ be an open bounded domain in $\mathbb{R}^2$. Let $V(y) = V(y_1, y_2)$ satisfy

$$\Delta_y V + \tilde{A}_1 \partial_{y_1} V + \tilde{A}_2 \partial_{y_2} V + \tilde{Q} V = 0 \quad \text{in} \quad \tilde{\Omega}. \tag{3.1}$$

Assume that $\tilde{A}_1, \tilde{A}_2 \in C^2(\bar{\tilde{\Omega}})$ and $\tilde{Q} \in L^\infty(\tilde{\Omega})$. Given $\omega \in \mathbb{R}^2$ with $|\omega| = 1$, we look for $V(y)$ of (3.1) having the form

$$V(y) = e^{y \cdot (\omega + i\omega^\perp)/h} (\tilde{L} + \tilde{R}), \tag{3.2}$$

where $\tilde{L}$ is independent of h and $\tilde{R}$ satisfies

$$\|\partial^\alpha \tilde{R}\|_{L^2(\tilde{\Omega})} \leq C h^{1-\alpha}, \quad \forall\ |\alpha| \leq 2. \tag{3.3}$$

To construct V having the form (3.2), (3.3), we follow the approach in [6] and [26] which are based on [4] and [16]. Note that the real part

of the phase function $y \cdot \omega$ is a limiting Carleman estimate. So if we set the semiclassical operator

$$P_h = h^2\Delta + h\tilde{A}_1(h\partial_{y_1}) + h\tilde{A}_2(h\partial_{y_2}) + h^2\tilde{Q},$$

then we can derive by combining a Carleman estimate and the Hahn-Banach theorem that

Theorem 3.1. [6] [26] *For h sufficiently small, for any $F \in L^2(\tilde{\Omega})$, there exists $W \in H_h^2(\tilde{\Omega})$ such that*

$$e^{-y\cdot\omega/h} P_h(e^{y\cdot\omega/h} W) = F$$

and $h\|W\|_{H_h^2(\tilde{\Omega})} \leq C\|F\|_{L^2(\tilde{\Omega})}$, where $\|W\|^2_{H_h^2(\tilde{\Omega})} = \sum_{|\alpha|\leq 2} \|(h\partial)^\alpha W\|^2_{L^2(\tilde{\Omega})}$ is the semiclassical H^2 norm.

Finding V of the form (3.2) is equivalent to solving

$$e^{-y\cdot(\omega+i\omega^\perp)/h} P_h(e^{y\cdot(\omega+i\omega^\perp)/h}(\tilde{L} + \tilde{R})) = 0 \quad \text{in} \quad \tilde{\Omega}.$$

We can compute that

$$e^{-y\cdot(\omega+i\omega^\perp)/h} P_h e^{y\cdot(\omega+i\omega^\perp)/h} = hT_\omega + P_h$$

where $T_\omega = 2(\omega + i\omega^\perp)\cdot\nabla + (\omega + i\omega^\perp)\cdot(\tilde{A}_1, \tilde{A}_2)$. Hence we want to find $\tilde{L}$, independent of h, so that

$$T_\omega \tilde{L} = 0 \quad \text{in} \quad \tilde{\Omega}. \tag{3.4}$$

The equation (3.4) is a system of the Cauchy-Riemann type. In fact, introducing the new variable $z = (z_1, z_2) = (\omega + i\omega^\perp)\cdot y$ and setting $\tilde{A}(\omega, z) = (\omega + i\omega^\perp)\cdot(\tilde{A}_1, \tilde{A}_2)$, (3.4) becomes

$$(4\partial_{\bar{z}} + \tilde{A})\tilde{L} = 0 \tag{3.5}$$

where $\partial_{\bar{z}} = (\partial_{z_1} + i\partial_{z_2})/2$. Having found $\tilde{L}$, $\tilde{R}$ is required to satisfy

$$e^{-y\cdot\omega/h} P_h(e^{y\cdot(\omega+i\omega^\perp)/h}\tilde{R}) = -e^{iy\cdot\omega^\perp/h} P_h\tilde{L}. \tag{3.6}$$

Note that $\|e^{iy\cdot\omega^\perp/h} P_h\tilde{L}\|_{L^2(\tilde{\Omega})} = O(h^2)$. Thus Theorem 3.1 implies that

$$\|e^{iy\cdot\omega^\perp/h}\tilde{R}\|_{H_h^2(\tilde{\Omega})} \leq Ch, \tag{3.7}$$

which leads to

$$\|\partial^\alpha\tilde{R}\|_{L^2(\tilde{\Omega})} \leq Ch^{1-|\alpha|} \quad \text{for} \quad |\alpha| \leq 2. \tag{3.8}$$

4. CGO solutions with general phases

In this section we will construct CGO solutions with more general phases for (1.1) from CGO solutions with linear phases given in the previous section. Without loss of generality, we choose $\omega = (1, 0)$ and $\omega^\perp = (0, 1)$, i.e., $y \cdot (\omega + i\omega^\perp) = y_1 + iy_2$. Denote $y = y_1 + iy_2$ and $x = x_1 + ix_2$. Let Ω_0 be an open subdomain of Ω. Suppose that A_1, $A_2 \in C^2(\bar{\Omega}_0)$ and $Q \in L^\infty(\Omega_0)$. Let $y = \rho(x) = y_1(x_1, x_2) + iy_2(x_1, x_2)$ be a conformal map in Ω_0, i.e., $\rho'(x) \neq 0$ for all $x \in \Omega_0$. Define $U(x) = V(y(x))$ and $\tilde{\Omega} = \rho(\Omega_0)$. By straightforward computations, we have

$$\begin{pmatrix} \partial_{x_1} \\ \partial_{x_2} \end{pmatrix} U = J(x) \begin{pmatrix} \partial_{y_1} \\ \partial_{y_2} \end{pmatrix} V \Big|_{y=\rho(x)} \quad \text{and} \quad \Delta_x U = \Delta_y V |\rho'(x)|^2,$$

where

$$J(x) = \begin{pmatrix} \partial_{x_1} y_1 & \partial_{x_1} y_2 \\ \partial_{x_2} y_1 & \partial_{x_2} y_2 \end{pmatrix}.$$

Suppose that ρ^{-1} exists on $\tilde{\Omega}$. Let $\hat{A}_1(y) = (A_1 \partial_{x_1} y_1 + A_2 \partial_{x_2} y_1) \circ \rho^{-1}(y)$, $\hat{A}_2(y) = (A_1 \partial_{x_1} y_2 + A_2 \partial_{x_2} y_2) \circ \rho^{-1}(y)$, and $\hat{Q}(y) = (Q \circ \rho^{-1})(y)$ and $g(y) = |(\rho' \circ \rho^{-1})(y)|^2$. Now if we choose $V(y)$ satisfying

$$\Delta_y V + g(y)^{-1} \hat{A}_1(y) \partial_{y_1} V + g(y)^{-1} \hat{A}_2(y) \partial_{y_2} V + g(y)^{-1} \hat{Q} V = 0 \quad \text{in } \tilde{\Omega}, \tag{4.1}$$

then $U(x)$ satisfies (1.1) in Ω_0. According to the construction given previously, let $V(y)$ be a solution of (4.1) having the form

$$V(y) = e^{(y_1 + iy_2)/h} (\tilde{L} + \tilde{R}),$$

where

$$\|\partial^\alpha \tilde{R}\|_{L^2(\tilde{\Omega})} \leq C h^{1-\alpha}, \quad \forall\ |\alpha| \leq 2.$$

Denote $y_1(x_1, x_2) = \varphi(x_1, x_2)$ and $y_2(x_1, x_2) = \psi(x_1, x_2)$. We then obtain CGO solutions for (1.1) in Ω_0:

$$U(x) = e^{(\varphi + i\psi)/h} (L + R)$$

with $L = \tilde{L} \circ \rho$, $R = \tilde{R} \circ \rho$, and

$$\|\partial^\alpha R\|_{L^2(\Omega_0)} \leq C h^{1-\alpha}, \quad \forall\ |\alpha| \leq 2. \tag{4.2}$$

Due to the conformality of ρ, φ and ψ are harmonic functions in Ω_0. Conversely, given any φ harmonic in Ω_0 with $\nabla \varphi \neq 0$ in Ω_0, we can find a harmonic conjugate ψ of φ in Ω_0 so that $\rho = \varphi + i\psi$ is conformal in Ω_0. The freedom of choosing φ plays a key role in our reconstruction method for the object identification problem. Actually, we will mainly focus on the level curves of φ. We give some concrete examples here.

Pick a point $x_0 \notin \bar{\Omega}$. It is no restriction to assume $x_0 = 0$. We now consider $\varphi_N = \mathrm{Re}(c_N x^N)$ for $N \geq 2$, where $c_N \in \mathbb{C}$ with $|c_N| = 1$. In the polar coordinates, $\varphi_N(r, \theta) = r^N \cos N(\theta - \theta_N)$ for some θ_N determined by c_N. We observe that $\varphi_N > 0$ in some open cone Γ_N with an opening angle π/N. The freedom of choosing θ_N (or, equivalently, c_N) allows us to "sweep" the domain Ω by Γ_N without moving the point x_0. This is quite useful in practice. Now assume that $\Gamma_N \cap \Omega \neq \emptyset$. The complex function $\rho_N(x) = c_N x^N = \varphi_N + i\psi_N$ is clearly conformal in Ω. In order to apply to the inverse problem, we want to shrink the opening angle of Γ_N by taking $N \to \infty$. However, there are two serious problems in doing so. On one hand, φ_N is periodic in the angular variable, which means that it is positive in some other cones with the same opening angle which also intersect Ω when N is large. Some level curves of φ_N for different N's are shown in Figure 4.1. This property of φ_N prohibits us from using corresponding CGO solutions with large N to the object identification problem. On the other hand, the complex function $\rho_N(x)$ fails to be injective in the whole domain Ω when N is large. To overcome those difficulties and construct useful CGO solutions in the whole domain Ω, we shall carry out the construction described above in a suitable Ω_0 and extend the constructed solutions to Ω by cut-off functions.

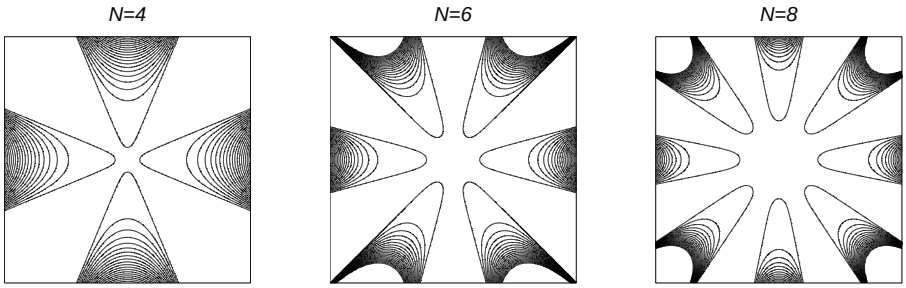

FIGURE 4.1. Some level curves of ϕ_N.

We now set

$$\Omega_0 := \Gamma_N \cap \Omega.$$

Then ρ_N is conformal in Ω_0 and is bijective from Ω_0 onto $\rho_N(\Omega_0)$. Therefore, we can find CGO solutions for (1.1) in Ω_0,

$$U_{N,h}(x) = e^{(\varphi_N + i\psi_N)/h}(L + R),$$

and the estimate (4.2) holds. So far we have only constructed special solutions for (1.1) in some particular subdomain of Ω. To get solutions in the whole domain Ω, we use a cut-off technique. For $s > 0$, let

$\ell_s = \{x \in \Gamma_N : \varphi_N = s^{-1}\}$. This is the level curve of ϕ_N in Γ_N. Let $0 < t < t_0$ such that

$$(\cup_{s\in(0,t)}\ell_s) \cap \Omega \neq \emptyset$$

and choose a small $\varepsilon > 0$. Define a cut-off function $\phi_{N,t}(x) \in C^\infty(\mathbb{R}^2)$ so that $\phi_{N,t}(x) = 1$ for $x \in \overline{(\cup_{s\in(0,t+\varepsilon/2)}\ell_s) \cap \Omega}$ and is zero for $x \in \bar{\Omega} \setminus (\cup_{s\in(0,t+\varepsilon)}\ell_s)$. We now define

$$U_{N,t,h}(x) = \phi_{N,t}e^{-t^{-1}/h}U_N = \phi_{N,t}e^{(\varphi_N - t^{-1} + i\psi_N)/h}(L + R)$$

for $x \in (\cup_{s\in(0,t+\varepsilon)}\ell_s) \cap \Omega$. So $U_{N,t,h}$ can be regarded as a function in Ω which is zero outside of Ω_0. We now take $f_{N,t,h} = U_{N,t,h}|_{\partial\Omega}$. We remark that $f_{N,t,h}$ can be used as the boundary data in the inverse problem. An obvious reason of using $f_{N,t,h}$ is that they are local.

Now we define a function $W := W_{N,t,h}$ satisfying

$$\begin{cases} \Delta W + A_1(x)\partial_{x_1}W + A_2(x)\partial_{x_2}W + Q(x)W = 0 \quad \text{in} \quad \Omega, \\ W = f_{N,t,h} \quad \text{on} \quad \partial\Omega. \end{cases} \tag{4.3}$$

We would like to compare $W_{N,t,h}$ with $U_{N,t,h}$. It turns out they differ only by an exponentially small term under some minor condition. This property play an essential role in our method for the inverse problem.

Lemma 4.1. *Assume that the boundary value problem*

$$\begin{cases} PU = 0 \quad \textit{in} \quad \Omega, \\ U = 0 \quad \textit{on} \quad \partial\Omega \end{cases} \tag{4.4}$$

has only trivial solution. Then there exist $C > 0$ and $\varepsilon' > 0$ such that

$$\|W_{N,t,h} - U_{N,t,h}\|_{H^2(\Omega)} \leq Ce^{-\varepsilon'/h} \tag{4.5}$$

for $h \ll 1$.

Proof. By setting $G := W_{N,t,h} - U_{N,t,h}$, we get that

$$\begin{aligned} PG &= P(W_{N,t,h} - U_{N,t,h}) \\ &= -\phi_{N,t}e^{-t^{-1}/h}PU_N + [\phi_{N,t}, P]e^{-t^{-1}/h}U_N \\ &= [\phi_{N,t}, P]e^{-t^{-1}/h}U_N \\ &= [\phi_{N,t}, P]e^{\varphi_N - t^{-1} + i\psi_N}(L + R) \end{aligned}$$

since $PU_N = 0$ in $(\cup_{s\in(0,t_0)}\ell_s) \cap \Omega$. Now we observe that $[\phi_{N,t}, P]$ is a first order differential operator with coefficients supported in

$$\overline{(\cup_{s\in(t+\varepsilon/2,t+\varepsilon)}\ell_s) \cap \Omega}.$$

So we have that

$$\|[\phi_{N,t}, P]e^{\varphi_N - t^{-1} + i\psi_N}(L + R)\|_{L^2(\Omega)} \leq C'e^{-\varepsilon'/h} \tag{4.6}$$

for some $C' > 0$ and $\varepsilon' > 0$. Note that $G = 0$ on $\partial\Omega$. Combining the regularity theorem, the triviality of (4.4), and (4.6) yields (4.5). □

Even though the solutions $W_{N,t,h}$ of (1.1) is not exactly in the form of complex geometrical optics, with the help of (4.1), they are exponentially close to $U_{N,t,h}$. Now we describe how to construct special solutions for some concrete systems given in Section 2 from $W_{N,t,h}$. For the conductivity equation (2.1), (1.1) is reduced to (2.2). For (2.2), we denote the corresponding $U_{N,t,h} = u_{N,t,h}$ and

$$u_{N,t,h} = \phi_{N,t} e^{(\varphi_N - t^{-1} + i\psi_N)/h}(1 + r),$$

where r satisfies (4.2). With $u_{N,t,h}$, we can solve for $w_{N,t,h}$ satisfying

$$\begin{cases} (\Delta + q)w = 0 & \text{in} \quad \Omega, \\ w = u_{N,t,h} & \text{on} \quad \partial\Omega. \end{cases} \tag{4.7}$$

The problem (4.7) has a unique solution since the boundary value problem for the corresponding conductivity equation has a unique solution. So Lemma 4.1 implies that

$$\|w_{N,t,h} - u_{N,t,h}\|_{H^1(\Omega)} \leq Ce^{-\varepsilon'/h}. \tag{4.8}$$

Returning to the conductivity equation, we see that $\gamma^{-1/2} w_{N,t,h}$ are solutions of (2.1).

For the isotropic elasticity and the Stokes system, we have $n = 3$ and (1.1) becomes respectively (2.7) and (2.10). We only discuss the isotropic elasticity here. The Stokes system can be treated similarly. Assume that the homogeneous boundary value problem (4.4) associated with (2.7) has only trivial solution. Thus Lemma 4.1 yields

$$\|W_{N,t,h} - U_{N,t,h}\|_{H^2(\Omega)} \leq Ce^{-\varepsilon'/h}.$$

We now express $U_{N,t,h} = \begin{pmatrix} v_{N,t,h} \\ b_{N,t,h} \end{pmatrix}$ and $W_{N,t,h} = \begin{pmatrix} w_{N,t,h} \\ g_{N,t,h} \end{pmatrix}$, where $v_{N,t,h}$, $w_{N,t,h}$ are two-dimensional vectors and $b_{N,t,h}$, $g_{N,t,h}$ are scalars. Hence, we obtain that

$$u_{N,t,h} = \mu^{-1/2} w_{N,t,h} + \mu^{-1} \nabla g_{N,t,h} - g_{N,t,h} \nabla \mu^{-1}$$

are solutions of (2.6) or (2.5) and $u_{N,t,h}$ satisfies

$$\|u_{N,t,h} - (\mu^{-1/2} v_{N,t,h} + \mu^{-1} \nabla b_{N,t,h} - b_{N,t,h} \nabla \mu^{-1})\|_{H^1(\Omega)} \leq Ce^{-\varepsilon'/h}.$$

5. Inverse problems

In this section we demonstrate how to use CGO solutions constructed previously in the object identification problem. To simplify our presentation, we will only discuss the case of identifying inclusions inside

of the domain Ω filled with known conductivity. This inverse problem has been extensively studied both theoretically and numerically. We refer to [7] for related references. Using our method, we can also treat the object identification problem for other systems. We shall report the results elsewhere.

Let D be an open bounded domain with C^1 boundary such that $\bar{D} \subset \Omega$ and $\Omega \setminus \bar{D}$ is connected. Assume $\gamma(x) \in C^2(\bar{\Omega})$ with $\gamma(x) > 0$ for all $x \in \bar{\Omega}$. The conductivity $\tilde{\gamma}(x)$ is a perturbation of γ described by $\tilde{\gamma}(x) = \gamma + \chi_D \gamma_1$, where χ_D is the characteristic function of D and $\gamma_1 \in C(\bar{D})$. We suppose

$$\gamma_1 \geq 0 \quad \text{on} \quad \bar{D}. \tag{5.1}$$

Then we have $\tilde{\gamma}(x) \geq c > 0$ almost everywhere in Ω. Let v be the solution of

$$\begin{cases} \nabla \cdot (\tilde{\gamma} \nabla v) = 0 \quad \text{in} \quad \Omega, \\ v = f \quad \text{on} \quad \partial\Omega. \end{cases} \tag{5.2}$$

The meaning of the solution to (5.2) is understood in the following way. Define

$$[w]_{\partial D} = \mathrm{tr}^+ w - \mathrm{tr}^- w$$

the jump of the function across ∂D, where tr^+ and tr^- denote respectively the trace of w on ∂D from inside and outside of D. For $f \in H^{3/2}(\partial\Omega)$, we define

$$\mathcal{V}_f = \{w \in H^2(D) \oplus H^2(\Omega \setminus \bar{D}) : w|_{\partial\Omega} = f, [w]_{\partial D} = 0, [\tilde{\gamma} \frac{\partial w}{\partial \nu}]_{\partial D} = 0\}.$$

We say that v is the solution of (5.2) if $v \in \mathcal{V}_f$ and $\nabla \cdot (\tilde{\gamma} v) = 0$ in D and $\Omega \setminus \bar{D}$. The Dirichlet-to-Neumann map is given as

$$\Lambda_D : f \to \tilde{\gamma} \frac{\partial v}{\partial \nu}|_{\partial\Omega},$$

where ν is the unit outer normal of $\partial\Omega$. The inverse problem is to determine the inclusion D from Λ_D. Here we are interested in the reconstruction question.

We begin with the following integral inequalities given in [15] (also see [7] for a proof).

Lemma 5.1. *Assume that* (5.6) *holds. Let* $f \in H^{3/2}(\partial\Omega)$ *and* u *be the unique solution of*

$$\begin{cases} \nabla \cdot (\gamma \nabla u) = 0 \quad \textit{in} \quad \Omega, \\ u = f \quad \textit{on} \quad \partial\Omega. \end{cases} \tag{5.3}$$

Define $\Lambda_0 : f \to \gamma \frac{\partial u}{\partial \nu}|_{\partial\Omega}$. *Then we have*

$$\int_{\partial\Omega} (\Lambda_D - \Lambda_0)\bar{f} \cdot f ds \leq \int_D \gamma_1 |\nabla u|^2 dx \tag{5.4}$$

and

$$\int_{\partial\Omega} (\Lambda_D - \Lambda_0)\bar{f} \cdot f ds \geq \int_D \frac{\gamma_1 \gamma}{\gamma + \gamma_1} |\nabla u|^2 dx. \tag{5.5}$$

For the inverse problem, we assume that for every $p \in \partial D$, there exists an $\epsilon > 0$ such that

$$\gamma_1 \geq \epsilon \quad \forall\ x \in D \cap B_\epsilon(p). \tag{5.6}$$

Let $x_0 \notin \bar{\Omega}$ and define the open cone Γ_N with $\Gamma_N \cap \Omega \neq \emptyset$ in terms of $\varphi_N = \mathrm{Re}(c_N(x - x_0)^N)$ ($f_N = c_N(x - x_0)^N$) as in Section 4. Likewise, we denote the level curve $\ell_s = \{x \in \Gamma_N : \varphi_N = s^{-1}\}$ for $s > 0$. For $\varepsilon > 0$ and $t > 0$, we take

$$f = f_{N,t,h} = \gamma^{-1/2} w_{N,t,h}|_{\partial\Omega} = \gamma^{-1/2} u_{N,t,h}|_{\partial\Omega}$$

where $w_{N,t,h}$ and $u_{N,t,h}$ are constructed previously. Note that $\gamma^{-1/2} w_{N,t,h}$ is the solution of (5.3). It should be noted that the Dirichlet condition f is localized in $\Gamma_N \cap \partial\Omega$ and becomes narrower as N gets bigger. This property is very useful in actual applications.

To construct the inclusion D, we rely on the quantity

$$E(N, t, h) := \int_{\partial\Omega} (\Lambda_D - \Lambda_0)\bar{f}_{N,t,h} \cdot f_{N,t,h} ds.$$

Clearly, this quantity is completely determined by the boundary data. From (5.1) and (5.5) we see that

$$E(N, t, h) \geq \int_D \frac{\gamma_1 \gamma}{\gamma + \gamma_1} |\nabla(\gamma^{-1/2} w_{N,t,h})|^2 dx \geq 0$$

for all N, t, h. We now prove the following important behavior of $E(N, t, h)$.

Theorem 5.2. *Let the curve ℓ_t be defined as above. Then we have:*
(i) *if $\ell_t \cap \bar{D} = \emptyset$ then there exist $C_1 > 0$, $\varepsilon_1 > 0$, and $h_1 > 0$ such that $E(N, t, h) \leq C_1 e^{-\varepsilon_1/h}$ for all $h \geq h_1$;*
(ii) *if $\ell_t \cap D \neq \emptyset$ then there exist $C_2 > 0$, $\varepsilon_2 > 0$, and $h_2 > 0$ such that $E(N, t, h) \geq C_2 e^{\varepsilon_2/h}$ for all $h \geq h_2$.*

Proof. To prove (i), we use the inequality (5.4) to obtain

$$E(N, t, h) \leq \int_D \gamma_1 |\nabla(\gamma^{-1/2} w_{N,t,h})|^2 dx \leq C \|w_{N,t,h}\|^2_{H^1(D)}. \tag{5.7}$$

With the help of (4.8), we can replace $w_{N,t,h}$ in (5.7) by $u_{N,t,h}$ with an error $O(e^{-\varepsilon'/h})$. Since $\ell_t \cap \bar{D} = \emptyset$, we have $\varphi_N - t^{-1} < 0$ for all $x \in \bar{D}$. So by the form of $u_{N,t,h}$ we immediately derive that

$$E(N,t,h) \leq Ce^{-\varepsilon_1/h}$$

for $h \geq h_1$.

To establish (ii), we first observe that $(\cup_{s\in(0,t)}\ell_s) \cap D \neq \emptyset$. So there exist $z \in \partial D$ and $\epsilon > 0$ such that the jump condition (5.6) holds and

$$\varphi_N - t^{-1} \geq \epsilon \quad \text{for all} \quad B_\epsilon(z) \cap D. \tag{5.8}$$

From (5.5) we get

$$\begin{aligned} E(N,t,h) &\geq \int_D \frac{\gamma_1\gamma}{\gamma+\gamma_1}|\nabla(\gamma^{-1/2}w_{N,t,h})|^2dx \\ &\geq C\epsilon\int_{D\cap B_\epsilon(z)}(|\nabla w_{N,t,h}|^2 + |w_{N,t,h}|^2)dx \\ &\geq C'\int_{D\cap B_\epsilon(z)}(|\nabla u_{N,t,h}|^2 + |u_{N,t,h}|^2)dx - C''e^{-\varepsilon'/h} \end{aligned} \tag{5.9}$$

Substituting the form of $u_{N,t,h}$ with the estimate (5.8) into (5.9) implies the statement of (ii). □

Furthermore, when ℓ_t touches the boundary of D, we can prove that

Theorem 5.3. *If $\ell_t \cap \partial D = \{p\}$ then $\liminf_{h\to 0} E(N,h,t) > 0$.*

Proof. In view of (5.6), we pick a sufficiently small $\epsilon > 0$ such that (5.6) is satisfied in $B_\epsilon(p) \cap D$ and $B_\epsilon(p) \cap D \subset (\cup_{s\in(t,t+\varepsilon/2)}\ell_s) \cap D$. So the cut-off function $\phi_{N,t} = 1$ on $B_\epsilon(p) \cap D$. We now introduce a new coordinate system $\Psi(x) = (y_1(x), y_2(x))$ near p with $y_2(x) = \varphi_N - t^{-1}$ such that ℓ_t becomes $y_2 = 0$ near p and $\tilde{D}_\epsilon := \Psi(B_\epsilon(p) \cap D)$ lies in $\{y_2 < 0\}$. We can choose a small cone C_p in $\tilde{D}_\epsilon$ with vertex p and the length of the axis is δ. Denote $J(y)$ the Jacobian of $\Psi^{-1}(y)$. Therefore,

using (5.9) we can estimate

$$\begin{aligned}
& E(N,t,h) \\
\geq\ & C' \int_{D\cap B_\epsilon(p)} (|\nabla u_{N,t,h}|^2 + |u_{N,t,h}|^2) dx - C'' e^{-\varepsilon'/h} \\
\geq\ & C' \int_{D\cap B_\epsilon(p)} (|\nabla (e^{(\varphi_N - t^{-1} + i\psi_N)/h}(1+r))|^2 + |e^{(\varphi_N - t^{-1} + i\psi_N)/h}(1+r)|^2) dx \\
& - C'' e^{-\varepsilon'/h} \\
\geq\ & \frac{\tilde{C}}{h^2} \int_{C_p} e^{2y_2/h} |J| dy_1 dy_2 - C'' e^{-\varepsilon'/h} \\
\geq\ & \frac{\tilde{C}'}{h^2} \int_{-\delta}^{0} e^{2y_2/h} y_2 dy_2 - C'' e^{-\varepsilon'/h} \\
>\ & 0 \quad \text{as} \quad h \to 0.
\end{aligned}$$

□

In view of Theorem 5.2 and 5.3, we are able to reconstruct some part of ∂D by looking into the asymptotic behavior of $E(N,t,h)$ for various t's. More precisely, let

$$t_{D,N} := \sup\{t \in (0,\infty) : \lim_{h\to 0} E(N,h,t) = 0\}$$

then if $t_{D,N} = \infty$ we have $\Gamma_N \cap D = \emptyset$. On the other hand, if $t_{D,N} < \infty$ then there exists a $p_{D,N} \in \ell_{t_{D,N}} \cap \partial D$.

By taking N arbitrarily large (the opening angle of Γ_N becomes arbitrarily small), we can reconstruct even more information of ∂D. A point p on ∂D is said to be *detectable* if there exists a semi-straight line l starting from p such that l does not intersect ∂D except p. For example, if D is star-shaped, every point of ∂D is detectable.

Corollary 5.4. *Every detectable point of ∂D can be reconstructed from Λ_D.*

Proof. Let p be a detectable point and l is the corresponding semi-straight line. We can choose that l is not tangent to $\partial\Omega$. Let L be the straight line containing l. Pick a point $x_0 \in L$ with $\frac{x_0-p}{|x_0-p|} = -\frac{z_0-p}{|z_0-p|}$ and $x_0 \notin \bar{\Omega}$. Let Γ_N be the cone with axis L and vertex x_0 whose opening angle is π/N. For any $N \in \mathbb{N}$, we construct $w_{N,t,h}$, $u_{N,t,h}$, and $f_{N,t,h}$ as above. So we can determine $E(N,t,h)$ from the measurement $\Lambda_D f_{N,t,h}$. Applying Theorem 5.2 and 5.3, we can determine $t_{D,N}$ so that $\ell_{t_{D,N}} \cap \partial D \neq \emptyset$. Choosing $N \to \infty$ and repeating the procedure yields the corollary. □

To end this section, we give an algorithm of our reconstruction method.

Step 1. Pick a point $x_0 \notin \bar{\Omega}$ (but close to $\bar{\Omega}$). Given $N \in \mathbb{N}$ and choose the cone Γ_N which intersects Ω.
Step 2. Start with $t > 0$ such that $\ell_t \cap \Omega \neq \emptyset$. Construct $u_{N,t,h}$ and determine the Dirichlet data $f_{N,t,h} = \gamma^{-1/2} u_{N,t,h}|_{\partial\Omega}$.
Step 3. Compute $E(N,t,h) = \int_{\text{supp } (f_{N,t,h})} (\Lambda_D - \Lambda_0) \bar{f}_{N,t,h} \cdot f_{N,t,h} ds$.
Step 4. If $E(N,t,h)$ is arbitrarily small, then increase t and repeat Step 2 and 3; if $E(N,t,h)$ is arbitrarily large, then decrease t and repeat Step 2 and 3.
Step 5. Repeat Step 4 to get a good approximation of ∂D in Γ_N.
Step 6. Move the cone Γ_N around x_0 by taking a different c_N in $\varphi_N = \text{Re}(c_N x^N)$. Repeat Step 2–5.
Step 7. Choose a larger N and a new cone Γ_N. Repeat Step 2–6.
Step 8. Pick a different x_0 and repeat Step 1–7.

6. Numerical results

We demonstrate some numerical results of our method in this section. Assume that the domain Ω is given by

$$\Omega = \{(x_1, x_2) : -1 < x_1 < 1, -1.01 < x_2 < -0.1\}.$$

We shall use the Dirichlet data localized on $\{(x_1, -1.01) : -1 < x < 1\}$. To set up $\rho_N(x)$, we consider $N = 4$. In our numerical computations, we use two sweeping schemes. In the first scheme, we fix the reference point x_0 and rotate the "probing cone" (the cone with the vertex at x_0 and the opening angle $\pi/4$). For the second one, we do not rotate the probing cone but move the reference points along the x-axis. More precisely, let the reference point $x_0 = (x_{0,1}, 0)$ for $-1 < x_{0,1} < 1$. In our first scheme, we fix $x_0 = (0,0)$ and rotate the probing cone determined by the shifted angle θ_N; while, in the second scheme, we consider different x_0's and choose $\theta_N = 0$. In other words, for both schemes, we have

$$\rho_N(x, x_0) = c_N(x_1 - x_{0,1} + ix_2)^N = e^{-iN\theta_N}(x_1 - x_{0,1} + ix_2)^N.$$

Thus, the probing fronts are level curves of $\phi_N := \text{Re}(\rho_N(x, x_0))$. Figure 6.1 shows some probing fronts of ϕ_N for $N = 4$.

We take the background conductivity $\gamma = 1$ and the conductivity inside the inclusion is 4, i.e, $\gamma_1 = 3$. For numerical experiments, we ignore the cut-off function and take

$$g_{N,x_0,h}|_{\partial\Omega} = \begin{cases} e^{\rho_N(x,x_0)/h}, & \text{for } (x_1, x_2) \in \partial\Omega_{\text{obs}}, \\ 0, & \partial\Omega \setminus \partial\Omega_{\text{obs}}, \end{cases}$$

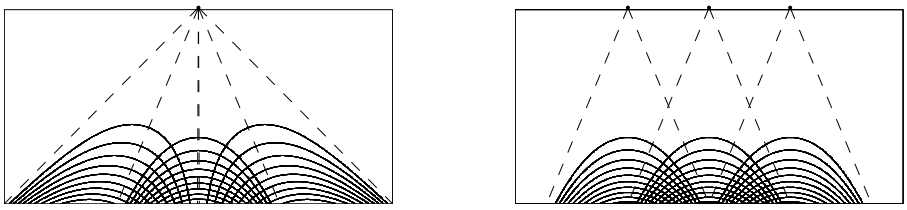

FIGURE 6.1. Probing fronts of our numerical method. In the first column, we consider the probing cone in three different angles. In the second column, we move the probing cone by taking three reference points. In our numerical method, we use ten different probing cones.

where $\partial\Omega_{\text{obs}}$ is determined by N, x_0, and θ_N. For example, for $N = 4$, $x_0 = (0, 0)$, $\theta_N = 0$,

$$\partial\Omega_{\text{obs}} = \{(x_1, x_2) : -1.01 \times \tan(\frac{\pi}{8}) < x_1 < 1.01 \times \tan(\frac{\pi}{8}),\ x_2 = -1.01\}.$$

Then for $t > 0$ the required Dirichlet data is given by $f = f_{N,t,h,x_0} = e^{-t^{-1}/h} g_{N,x_0,h}$. To get the synthetic data $\Lambda_0 f$ and $\Lambda_D f$, we need to solve the boundary value problems (5.2) and (5.3) with the Dirichlet condition f. To solve these forward problems, we use the pde toolbox with the finite element method in Matlab 7.0. Since we need to collect data on the bottom boundary of Ω, we refine the mesh there, see Figure 6.2.

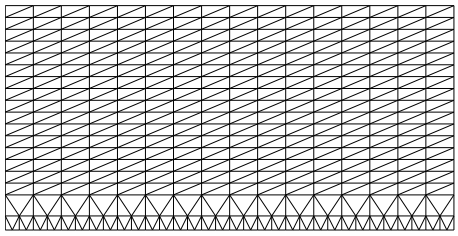

FIGURE 6.2. Example of our FEM meshes. The mesh has $2^m + 1$ nodes on the top boundary and $2^n + 1$ nodes on the lower boundary. This example is created with $m = 4$, $n = 6$. In solving our forward problems, we choose $m = 6$, $n = 12$.

To show the effect of noise to our method, we add appropriate noise to the synthetic data. We consider the form of noise given in [7]. To

be precise, let $\eta : [-1, 1] \mapsto \mathbb{C}$ be a random function defined by

$$\eta(s) = \sum_{k=-32}^{32} (a_k + ib_k)e^{iks\pi/2},$$

where $a_k, b_k \sim \mathcal{N}(0, 1)$ are normally distributed random numbers. The number 32 in η is chosen to roughly model a collection of 32 electrodes on the bottom boundary of Ω. Measurement noise is modeled by $\Lambda_D f$ by $\Lambda_D f + c\eta$ with

$$c = \frac{A\|\Lambda_D f\|_\infty}{\|\eta\|_\infty},$$

where $A > 0$.

Our strategy of reconstructing the inclusion is described as follows. We take appropriate h_1 and h_2 with $h_1 > h_2$ and choose a suitable number of probing fronts determined by t_j for $j = 1, \cdots, J$ with $t_j < t_{j+1}$. In each probing cone Γ_m, we construct the Dirichlet data f supported in the intersection of Γ_m and the bottom boundary of $\partial\Omega$ for every h_k and t_j, $j = 1, \cdots, J$, $k = 1, 2$, and $m = 1, \cdots, M$. We now evaluate $E_{j,k} := E(N, t_j, h_k)$ and determine t_n such that $E_{n+1,2} > E_{n+1,1}$. Then the region R_{Γ_m} defined by

$$R_{\Gamma_m} = \{x \in \Gamma_m : \phi_N(x) \leq t_n^{-1}\}$$

is the largest region in Γ_m which does not intersect the inclusion. So the region $R := \cup_m R_{\Gamma_m}$ is the one with absence of inclusion. Our numerical results for each sweeping scheme are shown in Figure 6.3 and Figure 6.4. To save computational time, we only show numerical results obtained from probing the region from one side (the bottom part of the boundary). Since our domain is rectangle, we can expect to obtain similar results when we probe the region from other sides. We believe that these numerical results are sufficient to demonstrate the applicability of our method.

7. Conclusion

In this work we present a framework of constructing special complex geometrical optics solutions for several systems of two variables that can be reduced to a system with the Laplacian as the leading term. Here we choose complex polynomials as phase functions. Using these special solutions, we design a novel algorithm to identify embedded objects with boundary measurements. One distinctive feature of our method is that we can probe the region using cones with as small opening angle as we wish. Theoretically, we are able to reconstruct the

exact geometry of the embedded object whose boundary points are all detectable. One typical example is the star-shaped object.

In the numerical experiments, we consider the case of inclusion embedded in a domain with homogeneous conductivity. The numerical results show that our method detects the location of inclusion quite well and is stable under measurements with (small) noise. For computational reasons, we only consider $N = 4$ and use two sweeping schemes separately. It is quite natural to consider higher N's and also combine two sweeping schemes into one. Of course, by doing so, we need to pay the price of increasing computational time.

Our method can be applied to classes of equations or even systems in two dimensions that can be reduced to the Laplacian on the top order part. Its flexibility and effectiveness gives us another technique that can potentially be used in real applications such as medical imaging or nondestructive evaluation.

ACKNOWLEDGMENTS

The program codes used in this work are modified from those used in [7]. We would like to thank H. Isozaki, T. Ide, S. Nakata, and S. Siltanen for generously sharing the codes with us. In completing the numerical results of this paper, the second author benefited from conversations with Z. Li, R. LeVeque, G. Nakamura, K.M. Shyue, and C.T. Wu.

References

[1] L. Borcea, *Electrical impedance tomography*, Inverse Problems, **18** (2002), R99-R136. Addendum, Inverse Problems, **19** (2003), 997-998.

[2] A. Calderón, *On an inverse boundary value problem*, Seminar on Numerical Analysis and its Applications to Continuum Physics, Soc. Brasileira de Matemática, Río de Janeiro (1980), 65-73.

[3] M. Cheney, D. Isaacson, and J. C. Newell, *Electrical impedance tomography*, SIAM Review, **41** (1999), no. 1, 85-101.

[4] D. Dos Santos Ferreira, C.E. Kenig, J. Sjöstrand, and G. Uhlmann, *Determining the magnetic Schrödinger operator from partial Cauchy data*, Comm. Math. Phys., to appear.

[5] G. Eskin and J. Ralston, *On the inverse boundary value problem for linear isotropic elasticity*, Inverse Problems, **18** (2002), 907-921.

[6] H. Heck, G. Uhlmann, and J.-N. Wang, *Reconstruction of obstacles immersed in an incompressible fluid*, Inverse Problems and Imaging, **1** (2007), 63-76.

[7] T. Ide, H. Isozaki, S. Nakata, S. Siltanen, and G. Uhlmann, *Probing for electrical inclusions with complex spherical waves*, to appear in Comm. Pure Appl. Math.

[8] M. Ikehata, *The enclosure method and its applications*, Analytic extension formulas and their applications (Fukuoka, 1999/Kyoto, 2000), 87-103, Int. Soc. Anal. Appl. Comput., 9, Kluwer Acad. Publ., Dordrecht, 2001.

[9] M. Ikehata, *A remark on an inverse boundary value problem arising in elasticity*, preprint.

[10] M. Ikehata, *Mittag-Leffler's function and extracting from Cauchy data*, Inverse problems and spectral theory, 41-52, Contemp. Math., **348**, Amer. Math. Soc., Providence, RI, 2004.

[11] M. Ikehata and S. Siltanen, *Electrical impedance tomography and Mittag-Leffler's function*, Inverse Problems, **20** (2004), 1325-1348.

[12] H. Isozaki, *Inverse spectral problems on hyperbolic manifolds and their applications to inverse boundary value problems in Euclidean space*, Amer. J. Math., **126** (2004), 1261-1313.

[13] H. Isozaki and G. Uhlmann, *Hyperbolic geometry and the local Dirichlet-to-Neumann map*, Advances in Math., **188** (2004), 294-314.

[14] J. Jordana, M. Gasulla, and R. Pallas-Areny, *Electrical resistance tomography to detect leaks from buried pipes*, Meas. Sci. Technol., **12** (2001), 1061-1068.

[15] H. Kang, J.K. Seo, and D. Sheen, *The inverse conductivity problem with one measurement: stability and estimation of size*, SIAM J. Math. Anal., **28** (1997), 1389-1405.

[16] C.E. Kenig, J. Sjöstrand, and G. Uhlmann, *The Calderón problem with partial data*, Ann. of Math., to appear.

[17] G. Nakamura and G. Uhlmann, *Global uniqueness for an inverse boundary problem arising in elasticity*, Invent. Math., **118** (1994), 457-474.

[18] G. Nakamura and G. Uhlmann, *Erratum: Global uniqueness for an inverse boundary value problem arising in elasticity*, Invent. Math. , **152** (2003), 205–207.

[19] A. Ramirez, W. Daily, D. LaBrecque, E. Owen, and D. Chesnut, *Monitoring an underground steam injection process using electrical resistance tomography*, Water Resources Research, **29** (1993), 73-87.

[20] A. Ramirez, W. Daily, A. Binley, D. LaBrecque, and D. Roelant, *Detection of leaks in underground storage tanks using electrical resistance methods*, J. Envir. Eng. Geophys., **1** (1996), 189-203.

[21] M. Salo and J.-N. Wang, *Complex spherical waves and inverse problems in unbounded domains*, Inverse Problems, **22** (2006), 2299-2309.

[22] L. Slater, L.; A. M. Binley, W. Daily, and R. Johnson, *Cross-hole electrical imaging of a controlled saline tracer injection*, Journal of Applied Geophysics, **44** (2000), 85- V102.

[23] J. Sylvester and G. Uhlmann, *A global uniqueness theorem for an inverse boundary value problem*, Ann. of Math.(2), **125** (1987), 153-169.

[24] G. Uhlmann, *Developments in inverse problems since Calderón's foundational paper*, Harmonic Analysis and Partial Differential Equations (*Essays in Honor of Alberto P. Calderón*), 295-345, The University of Chicago Press, Chicago, 1999.

[25] G. Uhlmann, *Commentary on Calderón's paper: On an inverse boundary value problem* (*Selecta, papers of Alberto P. Calderón*), edited by A. Bellow, C.E. Kenig and P. Malliavin.

[26] G. Uhlmann and J.-N. Wang, *Complex spherical waves for the elasticity system and probing of inclusions*, SIAM J. Math. Anal., to appear.
[27] Y. Zou and Z. Guo, *A review of electrical impedance techniques for breast cancer detection*, Med. Eng. Phys., 25 (2003), 79-90.

Department of Mathematics, University of Washington, Box 354305, Seattle, WA 98195-4350, USA.
E-mail address: gunther@math.washington.edu

Department of Mathematics, Taida Institute for Mathematical Sciences, and NCTS (Taipei), National Taiwan University, Taipei 106, Taiwan.
E-mail address: jnwang@math.ntu.edu.tw

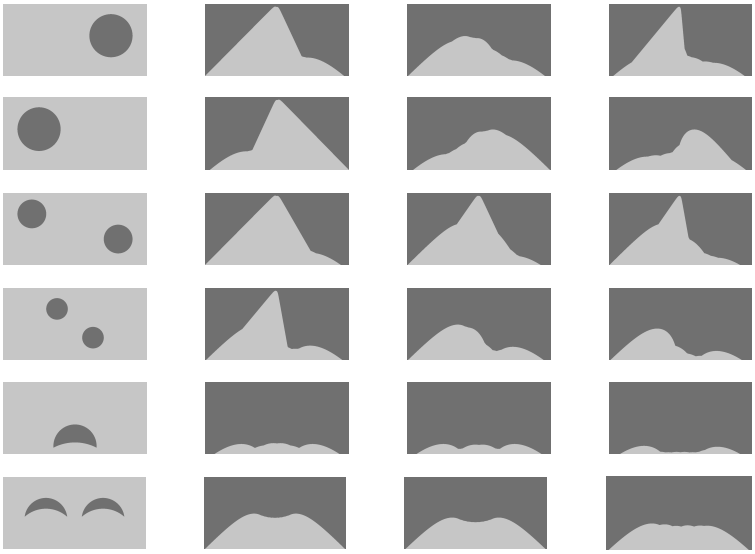

FIGURE 6.3. Numerical results of the first sweeping scheme. All black regions have the conductivity 4 and all gray regions have conductivity 1. The first column represents the actual location of inclusions. The second column is the theoretical reconstruction. The third column represents the reconstruction from noiseless synthetic data. The fourth column is the reconstruction from data with 0.01% noise.

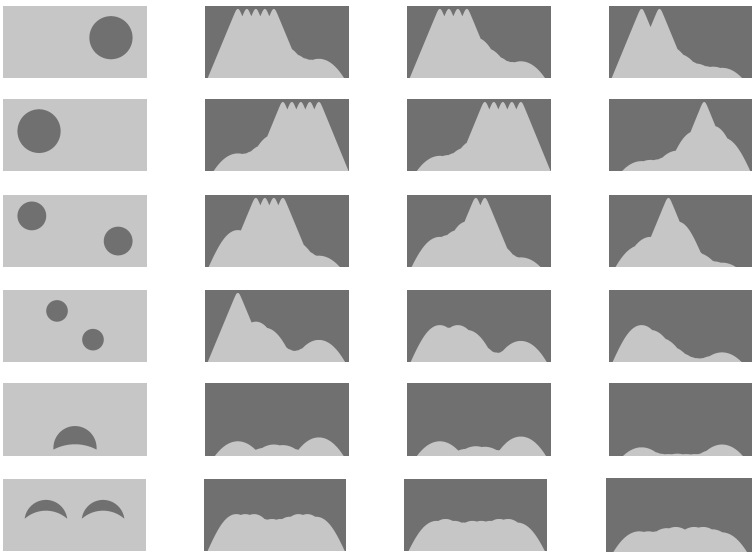

FIGURE 6.4. Numerical results of the second sweeping scheme. All black regions have the conductivity 4 and all gray regions have conductivity 1. The first column represents the actual location of inclusions. The second column is the theoretical reconstruction. The third column represents the reconstruction from noiseless synthetic data. The fourth column is the reconstruction from data with 0.01% noise.